

bilities. Third, the possibility of macroscopic states of the system is clearly indicated, although all detailed information about an ordered state is implicit in the undetermined function $f(\xi)$. It is conceivable that information about other types of macroscopic order (e.g., in momentum-space) would also be available from detailed knowledge of $n(\tau)$. The next step is, of course, to calculate the energy of an electron gas at high density with one or more appropriate trial functions for $K(\xi)$ in order to test the accuracy of the method against a known result. This will be done in a succeeding paper.

ACKNOWLEDGMENTS

The author wishes to acknowledge the kind help and valuable suggestions and criticisms from a number of people, particularly Professor T. Tanaka of Kyusyu University, Japan, Dr. M. Fisher of Kings College, London, Dr. R. Mazo and Professor J. E. Mayer of the Institute for Nuclear Studies, Chicago, Dr. M. S. Watanabe of I.B.M. Research Laboratories, Ossining, New York, and most particularly to Dr. R. H. Tredgold of U.C.N.W., Bangor, Wales without whose penetrating criticisms nothing whatsoever would have been achieved.

Quantum Statistical Theory of Electron Correlation*

ROBERT D. COWAN, *Los Alamos Scientific Laboratory, University of California, Los Alamos, New Mexico*

AND

JOHN G. KIRKWOOD, *Sterling Chemistry Laboratory, Yale University, New Haven, Connecticut*

(Received April 18, 1958)

The average electrostatic potential distribution about a given electron is calculated for a system of point-charge electrons embedded in a neutralizing continuum of positive charge. The calculation is classical, involving a Poisson equation of the Debye-Hückel type, except that the electron density is treated by means of Fermi-Dirac statistics as in the Thomas-Fermi theory of the atom. The calculated energy due to electrostatic interactions agrees with the quantum-mechanical exchange plus correlation energy over the observed range of metal valence-electron densities, $2 \leq r_s \leq 6$, but is too small at larger and smaller densities. (r_s is the electron-sphere radius in units of the Bohr radius.) The equilibrium density ($T = \mu = 0$) occurs at $r_s = 4.3$, at which point the compressibility is 69 per megabar. The electronic specific heat is linear in T at low temperatures and varies from 0.9 to 0.74 of the Sommerfeld value over the observed metal density range.

1. INTRODUCTION

A DEBYE-HÜCKEL, Thomas-Fermi (DHTF) theory of plasmas and liquid metals has recently been developed by Plock and Kirkwood.¹ The theory is similar to the Debye-Hückel theory of electrolyte solutions,² except that the charged particles are nuclei and electrons rather than positive and negative ions, and the behavior of the electrons is described in terms of Fermi-Dirac rather than Boltzmann statistics. The method of treating the electrons is similar to that of the Thomas-Fermi theory of the atom,³ but the DHTF theory automatically introduces a certain degree of correlation among the electrons due to their mutual electrostatic repulsion. It would be interesting to know how the correlation energy given by this theory would compare with that calculated quantum mechanically. However, the only quantum-mechanical calculation

with which a comparison can readily be made is for the case of free electrons moving in a uniform sea of positive charge; consequently, the DHTF theory is modified correspondingly in the discussion which follows.

2. THEORY

In the DHTF theory the thermodynamic functions are evaluated by considering the Debye charging process. For this purpose it is necessary to examine a hypothetical system in which each particle carries an arbitrary fraction λ of its true physical charge. Consider, then, a system consisting of electrons of (average) density n_0 each with a charge $-\lambda e$, embedded in a uniform neutralizing sea of positive charge of density

$$\lambda \rho_0 = \lambda e n_0. \quad (1)$$

Let $\psi_\lambda(r)$ be the average electrostatic potential at a distance r from any specific electron (due to *all* charges, including the electron in question). Then the potential energy of a second electron a distance r from the first is $-\lambda e \psi_\lambda(r)$, and the density of electrons at r is given

* Work performed under the auspices of the U. S. Atomic Energy Commission.

¹ R. J. Plock, thesis, Yale University, 1956; R. D. Cowan and J. G. Kirkwood, *J. Chem. Phys.* **29**, 264 (1958).

² P. Debye and E. Hückel, *Physik Z.* **24**, 185 (1923); see also R. Fowler and E. A. Guggenheim, *Statistical Thermodynamics* (Cambridge University Press, Cambridge, 1956), Secs. 904-913.

³ L. H. Thomas, *Proc. Cambridge Phil. Soc.* **23**, 542 (1927); E. Fermi, *Z. Physik* **48**, 73 (1928).

in the Thomas-Fermi approximation by

$$n(r) = \frac{2}{h^3} \int_0^\infty \frac{4\pi p^2 dp}{1 + \exp[(p^2/2m - \lambda e\psi - \mu)/kT]} \\ = 4\pi(2mkT/h^2)^{3/2} I_{3/2}(\eta), \quad (2)$$

where μ is the ideal chemical potential of the (uncharged) electron,

$$\eta = (\lambda e\psi + \mu)/kT, \quad (3)$$

and values of the integrals

$$I_m(\eta) \equiv \int_0^\infty y^m [1 + e^{y-\eta}]^{-1} dy \quad (4)$$

have been tabulated by McDougall and Stoner⁴ for $m = \frac{1}{2}$ and $\frac{3}{2}$. In the special case $\lambda = 0$, Eq. (2) reduces to

$$n_0 = 4\pi(2mkT/h^2)^{3/2} I_{3/2}(\mu/kT), \quad (5)$$

which serves to determine μ in terms of the average electron density.

The potential ψ and electron-density n about a specific electron are, using (1), related by means of the Poisson equation

$$\nabla^2 \psi_\lambda(r) \equiv -\frac{1}{r} \frac{\partial^2 (r\psi_\lambda)}{\partial r^2} = 4\pi\lambda e [n(r) - n_0], \quad (6)$$

with the boundary conditions

$$\lim_{r \rightarrow 0} r\psi_\lambda(r) = -\lambda e, \quad (7)$$

and

$$\lim_{r \rightarrow \infty} \psi_\lambda(r) = 0,$$

or from (2), (3), and (5)

$$\lim_{r \rightarrow \infty} n(r) = n_0. \quad (8)$$

The Helmholtz free energy per electron of the ideal (uncharged) electron gas is⁵

$$A_i \equiv E_i - TS_i = \mu - \frac{2}{3} E_i \\ = \mu - \frac{2}{3} kT I_{3/2}(\mu/kT) / I_{3/2}(\mu/kT), \quad (9)$$

where E_i is the average kinetic energy per electron and is calculated by adding a factor $p^2/2m$ to the integrand in (2). The free energy of the charged system is

$$A = A_i + A_e, \quad (10)$$

where A_e is the electrical work done in charging up the system at constant volume and temperature. This work can be readily calculated for the Debye charging process, in which at any given stage in the process each

particle possesses the same fraction λ of its final charge. The work done in charging each electron is

$$A_e = -e \int_0^1 \lim_{r \rightarrow 0} \left[\psi_\lambda(r) + \frac{\lambda e}{r} \right] d\lambda, \quad (11)$$

where $\psi_\lambda(r)$ is the potential about the electron at the temperature and average volume per electron of interest, and the potential $-\lambda e/r$ has been subtracted from ψ_λ so as to remove the electron self-energy. Any given element of positive charge is surrounded by a uniform positive-charge distribution; therefore the electron distribution about this element is also uniform on the average, and the average potential at the location of this element is nil. Thus the work done in charging the positive elements is zero and (11) gives the entire contribution to A_e .

Once A has been found from Eqs. (9) to (11), the pressure, entropy, and energy can be obtained from the thermodynamic relations

$$p = -(\partial A / \partial v)_T, \quad S = -(\partial A / \partial T)_v, \quad E = A + TS. \quad (12)$$

3. NUMERICAL METHODS

Numerical solutions of the Poisson equation were obtained in the following way. We introduce the units of length and energy

$$r_\lambda = \frac{h^2}{4\pi^2 m \lambda^2 e^2} \left(\frac{9\pi^2}{128} \right)^{1/3} = \frac{0.468479 \times 10^{-8}}{\lambda^2} \text{ cm}, \quad (13)$$

$$\theta_\lambda = 32m\lambda^4 e^4 h^{-2} = 22.0532\lambda^4 \text{ ev},$$

(which are the same as the usual Thomas-Fermi units except that e has been replaced by λe and Z has been set equal to unity), the dimensionless variables

$$x = r/r_\lambda \quad \text{and} \quad \theta = kT/\theta_\lambda, \quad (14)$$

and a potential function $\phi(x)$ defined by

$$\eta(x) = \theta^{-1} (4\epsilon)^{-2} \phi(x)/x, \quad (15)$$

where

$$4\epsilon = (6/\pi^2)^{1/3}.$$

Then using (2), (3), and (5) it can be seen that the Poisson equation (6) reduces to

$$\phi'' \equiv d^2\phi/dx^2 = \frac{3}{2} (4\epsilon)^3 x \theta^3 [I_{3/2}(\eta) - I_{3/2}(\eta_\infty)], \quad (16)$$

where $\eta_\infty \equiv \mu/kT$. The boundary conditions (7), (8), and (5) become

$$\phi(0) = -1, \quad (17)$$

$$\lim_{x \rightarrow \infty} (\phi/x) = (\phi/x)_\infty \equiv (4\epsilon)^2 \theta \eta_\infty. \quad (18)$$

In the special case $\theta \propto T \rightarrow 0$ in which we shall be especially interested, we see from (15) that $|\eta|$ is very large for all x . From the asymptotic expressions⁴ for $I_{3/2}$

⁴ J. McDougall and E. C. Stoner, *Trans. Roy. Soc. (London)* **A237**, 67 (1938).

⁵ See, for example, M. K. Brachman, *Phys. Rev.* **84**, 1263 (1951); or A. H. Wilson, *Thermodynamics and Statistical Mechanics* (Cambridge University Press, Cambridge, 1957), Sec. 6.3.

it follows that in the limit of zero temperature

$$I_{\frac{1}{2}}(\eta) \sim \frac{1}{2}\pi^{\frac{1}{2}}e^{\eta} \rightarrow 0, \quad \eta < 0, \quad (19a)$$

$$\theta^{\frac{2}{3}}I_{\frac{1}{2}}(\eta) \sim \frac{2}{3}(\theta\eta)^{\frac{2}{3}} = \frac{2}{3}(4\epsilon)^{-\frac{2}{3}}(\phi/x)^{\frac{2}{3}}, \quad \eta > 0, \quad (19b)$$

so that the differential equation (16) becomes

$$\phi'' = -x(\phi/x)_{\infty}^{\frac{2}{3}}, \quad \phi < 0, \quad (20a)$$

$$\phi'' = x[(\phi/x)^{\frac{2}{3}} - (\phi/x)_{\infty}^{\frac{2}{3}}], \quad \phi > 0. \quad (20b)$$

Except for the final term on the right (and the different boundary conditions), Eqs. (20b) and (16) are of course identical with the familiar Thomas-Fermi equations for zero and nonzero temperatures, respectively.⁶ [Actually, the zero-temperature results quoted below were calculated by using Eq. (16) with $kT = 2.2 \times 10^{-12}$ ev; i.e., $\theta = 10^{-13}/\lambda^4$.]

Regardless of the value of θ , it follows from (15) and (17) that for small x , $\eta(x)$ is a large negative number and that $I_{\frac{1}{2}}(\eta) \ll I_{\frac{1}{2}}(\eta_{\infty})$. Thus for small x the differential equation (16) integrates to

$$\phi(x) = -1 + bx - \frac{1}{4}(4\epsilon)^{\frac{2}{3}}\theta^{\frac{2}{3}}I_{\frac{1}{2}}(\eta_{\infty})x^3, \quad (21)$$

where b is a constant whose value must be chosen so as to satisfy the boundary condition (18).

For very large x , $\eta \approx \eta_{\infty}$ from (18), and (16) can be written approximately

$$\begin{aligned} \phi'' &\sim \frac{2}{3}(4\epsilon)^{\frac{2}{3}}x\theta^{\frac{2}{3}}(\partial I_{\frac{1}{2}}/\partial\eta)_{\eta_{\infty}}(\eta - \eta_{\infty}) \\ &= 6\epsilon\theta^{\frac{2}{3}}(\partial I_{\frac{1}{2}}/\partial\eta)_{\eta_{\infty}}[\phi - (\phi/x)_{\infty}x]. \end{aligned} \quad (22)$$

In view of the boundary condition (18), the integral of this expression is

$$\phi(x) \sim (\phi/x)_{\infty}x - Be^{-Kx}, \quad (23)$$

where

$$K^2 = 6\epsilon\theta^{\frac{2}{3}}(\partial I_{\frac{1}{2}}/\partial\eta)_{\eta_{\infty}}. \quad (24)$$

The procedure used for integrating the general equation (16) was, then, the following: For given values of the temperature T and average electron density n_0 , the value of $\eta_{\infty} = \mu/kT$ was obtained by an iterative

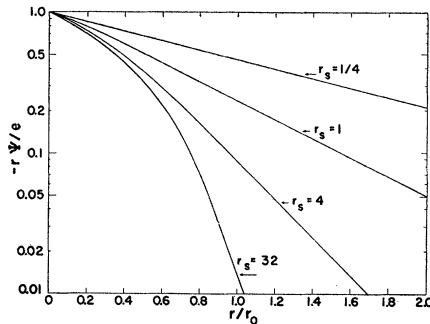


FIG. 1. The average potential distribution about a specific electron for various average electron densities at zero temperature ($\lambda = 1$).

⁶ Feynman, Metropolis, and Teller, Phys. Rev. 75, 1561 (1949), Eqs. (1) and (15).

solution of (5) and the value of K calculated from (24), $I_{\frac{1}{2}}(\eta)$ being evaluated by means of asymptotic series expansions for large $|\eta|$ and cubic table interpolation for small $|\eta|$.⁴ For a given value of λ , θ was calculated from (14), and then the solution of (16) found for small x from (21), using a guessed value of b . Integration was advanced to large x by means of a difference method, and the numerical solution then compared with the analytical solution (23) by evaluating B to match the numerical value of ϕ and then comparing the slopes of the two solutions. The value of b was then repeatedly modified until the two slopes agreed. Using IBM type 704 digital calculators, integration for one value of b required about one second, with about fifteen cycles being sufficient to iterate to a value of b constant to seven or eight significant figures.

The value of b was thus determined for twelve values of λ and then A_e calculated with the aid of Simpson's Rule by writing (11) in the form

$$A_e = -(e^2/2a_0)(128/9\pi^2)^{\frac{1}{2}} \int_0^1 \lambda^2 [b - (\phi/x)_{\lambda}]_{\lambda} d(\lambda^2), \quad (25)$$

where the relations (3), (13), (15), and (21) have been used, and $a_0 = \hbar^2/me^2$ is the first Bohr radius for hydrogen.

4. RESULTS

A. Zero-Temperature Electron Distribution and Potential

Before discussing the numerical results it is of some interest to examine the asymptotic form of the potential $\psi(r)$, which from (3), (15), and (23) can be written in the form

$$\psi(r) \sim (-B\lambda e/r)e^{-k_{\lambda}r}, \quad (26)$$

where $k_{\lambda} = K/r_{\lambda}$. In the high-temperature, low-density limit, then from (19a) $(\partial I_{\frac{1}{2}}/\partial\eta)_{\eta_{\infty}} = I_{\frac{1}{2}}(\eta_{\infty})$, and from (5) and (24), it may readily be seen that

$$k_{\lambda} = (4\pi\lambda^2 e^2 n_0/kT)^{\frac{1}{2}}, \quad (27)$$

which is of course identical with the standard Debye-Hückel result.²

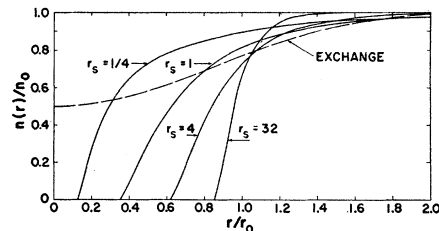


FIG. 2. The electron-density radial distribution function for various average electron densities at zero temperature ($\lambda = 1$). The dashed curve is the quantum-mechanical (exchange) result.

TABLE I. Numerical results (for $\lambda=1$ where pertinent).

r_s	$(\phi/x)_\infty$	b	B [Eq. (26)]	$r_s E_e = r_s A_s^0$ (ry)	$r_s E_p$ [Eq. (33)] (ry)	p^0 (megabars)	a [Eq. (42)] (ry) ⁻¹	kT_{\max}^a (ev)
0.0025	2.60870×10^5	2.60897×10^6						
0.025	2.60870×10^3	2.61740×10^3						
0.0625	4.17391×10^2	4.22826×10^2						
0.125	1.04348×10^2	1.08100×10^2						
0.25	2.60870×10^1	2.86097×10^1	1.0155	-0.4942	-0.7123	5.22×10^4	0.005	20
0.5	6.52174×10^0	8.14365×10^0	1.0455	-0.6596	-0.9159	1.58×10^3	0.012	10
1	1.63043×10^0	2.61170×10^0	1.1318	-0.8424	-1.1082	4.49×10^1	0.031	5
2	4.07609×10^{-1}	9.65348×10^{-1}	1.3658	-1.0194	-1.2598	1.05×10^0	0.069	2
4	1.01902×10^{-1}	4.03446×10^{-1}	2.0189	-1.1698	-1.3622	5.80×10^{-3}	0.127	0.5
8	2.54755×10^{-2}	1.83133×10^{-1}	4.1505	-1.2843	-1.4244	-1.71×10^{-3}	0.212	0.1
16	6.36889×10^{-3}	8.71525×10^{-2}	14.1110	-1.3645	-1.4598	-1.77×10^{-4}		
32	1.59222×10^{-3}	4.25208×10^{-2}	95.6882	-1.4173	-1.4792	-1.36×10^{-5}		

^a Approximate maximum temperature at which the temperature dependence of A_s is given within five percent by Eq. (42).

In the opposite limit of zero temperature, then from (19b) the form

$$(\partial I_{3/2} / \partial \eta)_{\eta_\infty} = \frac{3}{2} I_{3/2}(\eta_\infty) / \eta_\infty = (\frac{3}{2} kT / E_0) I_{3/2}(\eta_\infty),$$

where E_0 is the kinetic energy $p_0^2 / 2m$ of an electron at the top of the Fermi distribution. Thus, in this case, the screening constant may be written⁷

$$k_\lambda = (12\pi\lambda^2 m e^2 n_0 / p_0^2)^{1/2} = (16/3\pi^2)^{1/2} \lambda r_s^{1/2} k_0 = 0.8145 \lambda r_s^{1/2} k_0, \quad (28)$$

where $r_s = r_0 / a_0$ is the electron-sphere radius in units of a_0 , i.e., $n_0^{-1} = \frac{4}{3}\pi r_0^3$, and k_0 is the maximum wave number of an electron, $k_0 = p_0 / \hbar = (9\pi/4)^{1/2} / r_s a_0$. The coefficient 0.8145 (for $\lambda=1$) is much greater than the quantum-mechanical value $2^{-3/2} = 0.3536$ derived by Pines.⁷ However, this does not necessarily imply that the Thomas-Fermi model overestimates the effectiveness of the screening and overestimates the electron correlation energy, for it must be remembered that (26) is only an asymptotic expression and that B is not necessarily unity. Indeed, the numerical results given in Table I and Fig. 1 show that $B > 1$ and that the screening is considerably less effective than would be expected from (28) alone.

The solid curves in Fig. 2 show the electron-density radial distribution functions corresponding to the potential curves of Fig. 1.

B. Zero-Temperature Energy

The zero-temperature energy of a free-electron gas has been investigated quantum-mechanically by Wigner,⁸ by Bohm and Pines,⁹ and by Gell-Mann and Brueckner.¹⁰ The energy per electron can be written in

⁷ D. Pines, *Solid-State Physics* edited by F. Seitz and D. Turnbull (Academic Press, Inc., New York, 1955), Vol. 1, pp. 377, 386 ff., and 394.

⁸ E. Wigner, *Phys. Rev.* **46**, 1002 (1934).

⁹ D. Pines, *Solid-State Physics* edited by F. Seitz and D. Turnbull (Academic Press, Inc., New York, 1955), Vol. 1, pp. 367-406.

¹⁰ M. Gell-Mann and K. A. Brueckner, *Phys. Rev.* **106**, 364 (1957).

$$E = E_F + E_{\text{exch}} + E_{\text{corr}} = \frac{2.210}{r_s^2} - \frac{0.916}{r_s} + E_{\text{corr}}, \quad (29)$$

where the coefficients give energies in Rydbergs, the first term is the Fermi energy (the kinetic energy of the free electron gas without electrostatic interactions), the second is the exchange energy (i.e., the potential energy in the Hartree-Fock approximation), and the third is the correlation energy (the balance of the energy calculated by any more accurate method).

At zero temperature, the Helmholtz free energy and the internal energy are equal, and so the DHTF expression (10) may be written in this case

$$E = E_i + E_e. \quad (30)$$

The energy of the ideal gas, E_i , is just its kinetic energy and is identical with the first term of (29). The charging energy, E_e , has been calculated on an essentially classical basis and cannot be broken up into an exchange and a correlation energy, and so must be compared with the sum $E_{\text{exch}} + E_{\text{corr}}$ in Eq. (29).

These various energies (multiplied by r_s) are shown in Fig. 3, where E_{corr} has been taken to be given by Gell-Mann and Brueckner's expression

$$E_{\text{corr}} = 0.0622 \ln r_s - 0.096 \text{ ry}, \quad (31a)$$

for $r_s < 1$, and by the corrected Wigner approximation formula⁹

$$E_{\text{corr}} = -0.88 / (r_s + 7.8) \text{ ry} \quad (31b)$$

for $r_s \geq 1$. The difference between E_e and $E_{\text{exch}} + E_{\text{corr}}$ is surprisingly small over the range $2 \leq r_s \leq 6$ corresponding to observed metal-valence-electron densities, and in fact lies at most points within the twenty percent uncertainty which Wigner estimated for the expression (31b).¹¹ At smaller values of r_s , the agreement

¹¹ The difference between the two curves at large r_s arises from the fact that DHTF is strictly a fluid theory, whereas the physical system is expected to undergo a phase change from an electron gas to an electron lattice at some large value of r_s . The formula

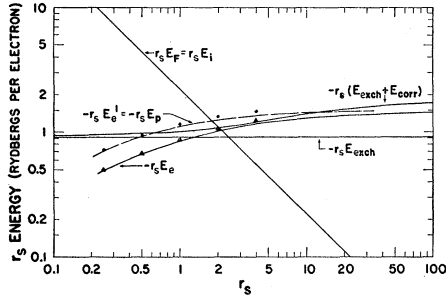


FIG. 3. Dependence on electron density of the various electronic energies at zero temperature. The energy of the ideal gas is E_F ; the additional energy due to electrostatic interactions is $E_{\text{exch}} + E_{\text{corr}}$ in the quantum-mechanical calculation and E_e in the DHTF theory. In the DHTF case, the potential energy is E_p , and the total kinetic energy is $E_F + E_e - E_p$; the circles and triangles denote results obtained when an exchange term is included in the Fermi-Dirac energy distribution function.

becomes increasingly poorer, as one might well expect: For small r_s the asymptotic expression (26) is valid to small values of $r(B \approx 1)$, Fig. 1, and so $|E_e|$ is much greater than $|E_{\text{corr}}|$; but the electron correlation in the DHTF theory is purely electrostatic in origin, and includes nothing analogous to the Pauli-principle correlation which gives rise to the exchange energy in the quantum-mechanical theories.

The situation can be examined in somewhat greater detail with the aid of Fig. 2, where the solid curves represent electrostatic correlation in the absence of exchange effects, and the dashed curve¹²

$$\frac{n(r)}{n_0} = 1 - \frac{9}{2} \left(\frac{\sin x - x \cos x}{x^3} \right)^2, \quad x = \left(\frac{9\pi}{4} \right)^{\frac{1}{2}} \frac{r}{r_0}, \quad (32)$$

(which is independent of r_s) gives the exchange correlation in the absence of electrostatic effects. It is evident that the electrostatic correlation is more effective than the statistical for r_s greater than about unity. From this follows the fact illustrated in Fig. 3 that the DHTF energy is greater (in magnitude) than the exchange energy for $r_s > 1.3$.

Though the DHTF theory as described above provides no statistical contribution to the correlation, there are two obvious modifications of the theory through which one might try to simulate the effects of such a contribution on the energy.

First, it may be noted that Pauli-principle correlation

(31b) has therefore been chosen so that $E_{\text{exch}} + E_{\text{corr}}$ extrapolates to the value $-1.8/r_s$ for a bcc lattice. It would perhaps be fairer (at least out to the value of r_s at which the phase change occurs) to compare the DHTF results with Wigner's original formula which extrapolates to the gas value $-1.5/r_s$; if this is done, the two curves agree within two percent for $r_s > 3.5$.

¹² W. Wigner and F. Seitz, *Phys. Rev.* **43**, 804 (1933); **46**, 509 (1934). Or F. Seitz, *Modern Theory of Solids* (McGraw-Hill Book Company, Inc., New York, 1940), pp. 240 ff. The exchange curve has the value $n(0)/n_0 = 1/2$, because the Pauli principle affects only half the electrons (those with spin parallel to that of the electron at the origin). All curves of Fig. 2 correspond to a "hole" of exactly one electron.

is independent of the electron charge. This sort of behavior can be incorporated easily into the DHTF theory by using for all λ the electron distribution which is calculated for $\lambda = 1$ ¹³; i.e., by replacing (25) with¹⁴

$$E_e^1 = E_p = - (e^2/2a_0) (128/9\pi^2)^{\frac{1}{2}} [b - (\phi/x)_\infty]_{\lambda=1}. \quad (33)$$

Values of E_e^1 calculated from this expression at zero temperature are plotted as the dashed curve in Fig. 3. It may be seen that the magnitude of E_e^1 is indeed greater than that of E_e . However, the moderate improvement at small r_e is accompanied by poorer agreement at larger r_e , and since the modification is quite artificial at best, it does not seem worth while to consider it further.

A second approach is to include an exchange term in the distribution function (2) in the same manner as is done in the Thomas-Fermi-Dirac theory of the atom.¹⁵ At zero temperature, this leads to equations identical with (20) except that $[\epsilon + (\phi/x)^{\frac{1}{2}}]^3$ appears everywhere in place of $(\phi/x)^{\frac{3}{2}}$. Although this modification produces rather large changes in b and in $(\phi/x)_\infty$, the changes in $b - (\phi/x)_\infty$ prove to be rather small. Since Eqs. (9), (10), (25), and (33) remain unchanged, the results (shown by means of circles and triangles in Fig. 3) do not differ greatly from those obtained without the exchange term, except that the ϵ makes it impossible to calculate for an electron density less than 7.35×10^{21} electrons/cc ($r_s > 6.03$). Therefore, this second modification is also unsatisfactory, and all further results given below are for the original form of the theory.

C. Zero-Temperature Pressure

At zero temperature, the electron pressure is given by (12) and (30) as $p = -\partial(E_i + E_e)/\partial v$, which from (29) may be written

$$pv = \frac{2}{3} E_i - \frac{1}{3} E_e \frac{\partial \ln(-E_e)}{\partial \ln r_s} = \frac{1.473}{r_s^2} + \frac{1}{3} E_e \left[1 - \frac{\partial \ln(-r_s E_e)}{\partial \ln r_s} \right] \text{ry.} \quad (34)$$

The necessary derivatives were evaluated from Fig. 3, and the results are shown both the in Fig. 4 for DHTF energy E_e and the quantum mechanical energy $E_{\text{ex}} + E_{\text{corr}}$. For comparison, the contribution to the pressure of the Fermi energy only is also shown.

For both the quantum mechanical and DHTF calculations, the equilibrium electron density corresponds to r_s equals about 4.2; this is roughly in the middle of the observed range $2 \leq r_s \leq 6$ of metal-valence-

¹³ This is an overestimate of the effect inasmuch as the Pauli principle applies only to electrons of the same spin, but is an underestimate at small r_s in that the electrostatic correlation even at $\lambda = 1$ is much less than the Pauli correlation.

¹⁴ The symbol E_p is also used, because it can be seen that this expression is just the potential energy of the system; see Sec. 4C.

¹⁵ R. D. Cowan and J. Ashkin, *Phys. Rev.* **105**, 144 (1957).

electron densities. As is well known, the free-electron pressure in this range is quite large ($p_i=39100$ atmos at $r_s=4.2$) so that the electrostatic effect is quite sizeable.

At first glance it might appear from (34) that the virial theorem for Coulombic forces,

$$pv = \frac{2}{3}E_{\text{kinetic}} + \frac{1}{3}E_{\text{potential}}, \quad (35)$$

is satisfied by neither the quantum mechanical nor the DHTF results since neither $r_s E_{\text{corr}}$ nor $r_s E_e$ is independent of r_s . However, it must be remembered that $E_F = E_i$ is the kinetic energy of the *uncharged* system, and that E_{corr} and E_e include not only electrostatic potential energy but also a change in the kinetic energy brought about by the charging process.

In fact, in the DHTF case the potential energy is just the quantity E_p defined by (33) and plotted as the dashed line in Fig. 3. The contribution of E_e to the kinetic energy is thus $E_e - E_p$, and the virial theorem (35) may be written

$$pv = \frac{2}{3}(E_i + E_e - E_p) + \frac{1}{3}E_p \\ = \frac{2}{3}E_i + \frac{1}{3}E_e + \frac{1}{3}(E_e - E_p). \quad (36)$$

The last term in this expression is by no means negligible (as can be seen from Fig. 3), and its value agrees with that of the corresponding term of (34) to within 3 or 4% over the entire range $0.25 \leq r_s \leq 32$. Since the graphical differentiation involved is subject to at least that large an error, the virial theorem may be considered as having been verified numerically.

The virial theorem can in fact be established analytically (at zero temperature) in the following way¹⁶: Suppose that the values of $(\phi/x)_\infty$ and of b , Eq. (25), are known for all values of λ for some particular volume, v_1 , per electron. Let any other volume, v_c , be expressed in terms of v_1 by means of a linear-scale-factor c^2 :

$$v_c = c^6 v_1. \quad (37)$$

Then from (5), (13), (14), and (19) it follows that at zero temperature and at volume v_c

$$n_0 = c^{-6} v_1^{-1} \propto (\theta_\lambda \theta)^{\frac{3}{2}} I_{\frac{3}{2}}(\eta_\infty) \propto \lambda^6 (\phi/x)_\infty^{\frac{3}{2}}.$$

Thus $(\phi/x)_\infty$ is a function only of $c\lambda$, so that

$$[(\phi/x)_\infty]_{\lambda, v_c} = [(\phi/x)_\infty]_{c\lambda, v_1}. \quad (38)$$

Since the solution of (20) depends only on the value of $(\phi/x)_\infty$, it follows that a relation similar to (38) holds for b . Consequently, at zero temperature (25) can be

¹⁶ This proof is similar in some respects to that for the Thomas-Fermi atom: V. Fock, *Physik Z. Sowjetunion* **1**, 747 (1932); H. Jensen, *Z. Physik* **111**, 373 (1939). The proof can be extended to nonzero temperatures in a manner similar to that used for the unmodified DHTF theory; Cowan and Kirkwood, reference 1.

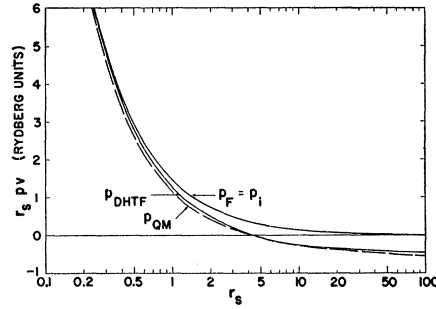


FIG. 4. The zero-temperature pressure of an ideal electron gas, and the pressure including interactions calculated both quantum-mechanically and from the DHTF theory.

written

$$E_e(v_c) = K \int_0^1 \lambda^2 [b - (\phi/x)_\infty]_{\lambda, v_c} d(\lambda^2) \\ = K c^{-4} \int_0^{c^2} c^2 \lambda^2 [b - (\phi/x)_\infty]_{c\lambda, v_1} d(c^2 \lambda^2),$$

where K is the constant in (25). The contribution of $E_e(v_c) \equiv E_e(c^6 v_1)$ to the pressure is therefore

$$p_e v_c = -v_c \frac{\partial E_e(c^6 v_1)}{\partial (c^6 v_1)} = -\frac{c}{6} \frac{\partial E_e(c^6 v_1)}{\partial c} \\ = \frac{2}{3} E_e(v_c) - \frac{1}{3} K [b - (\phi/x)_\infty]_{c, v_1} \\ = \frac{2}{3} E_e(v_c) - \frac{1}{3} K [b - (\phi/x)_\infty]_{1, v_c}.$$

Since the final term here is just $-\frac{1}{3} E_p(v_c)$ from (33) and since the contribution of $E_e(v_c)$ to $p v_c$ was shown in (34) to be $\frac{2}{3} E_i$, the proof of (36) is complete.

The compressibility of the DHTF system at $T = p = 0$ (obtained by graphical differentiation of Fig. 4 at $r_s = 4.3$) is

$$\kappa \equiv -v^{-1} (\partial v / \partial p)_T = 69 \text{ (megabar)}^{-1}.$$

As might be anticipated, this value is considerably larger than experimental compressibilities of the alkali elements (8.7 for Li to 49.3 for Cs), and much larger than those for most other elements [of the order of 1 (megabar)⁻¹].¹⁷

D. Low-Temperature Specific Heat

From Eqs. (5) and (9) it can be shown with the aid of the asymptotic expressions for $I_m(\eta)$,¹⁸ that to the second order in T

$$A_i = \frac{3}{5} \mu_0 - \frac{1}{4} \pi^2 (kT)^2 / \mu_0, \quad (39)$$

¹⁷ J. J. Gilvarry, *J. Chem. Phys.* **23**, 1925 (1955); J. Waser and L. Pauling, *J. Chem. Phys.* **18**, 747 (1950).

¹⁸ See reference 4, or J. E. Mayer and M. G. Mayer, *Statistical Mechanics* (John Wiley and Sons, Inc., New York, p. 1940), 385.

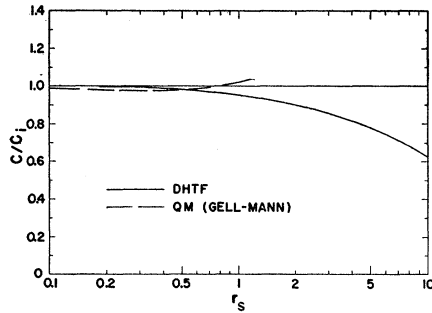


FIG. 5. Ratio of the low-temperature specific heat of the electron gas with interactions to the Sommerfeld value C_i .

where

$$\mu_0 = \frac{\hbar^2}{8m} \left(\frac{3n_0}{\pi} \right)^{\frac{2}{3}} = \left(\frac{9\pi}{4} \right)^{\frac{2}{3}} \frac{me^4}{2\hbar^2 r_s^2}. \quad (40)$$

From (39) and (12) one obtains the familiar Sommerfeld value for the specific heat

$$(C_v)_i = \frac{\partial E_i}{\partial kT} = \frac{\pi^2 kT}{2 \mu_0} = \left(\frac{4\pi^2}{9} \right)^{\frac{2}{3}} \frac{\hbar^2 r_s^2 kT}{me^4} = 1.3406 r_s^2 kT, \quad (41)$$

the coefficient being for kT in Rydbergs. At low temperatures, the calculated values of A_e can be written in a form analogous to (39):

$$A_e = A_e^0 + a(r_s kT)^2, \quad (42)$$

the values of A_e^0 and a being given in Table I. The low-temperature specific heat of the electrons is thus given by

$$C_v / (C_v)_i = 1 - 2ar_s^2 kT / (C_v)_i = 1 - 1.4919a. \quad (43)$$

This ratio is compared in Fig. 5 with the zero-temperature expression

$$C_v / (C_v)_i = [1 + 0.083r_s(-\ln r_s - 0.203)]^{-1}, \quad (44)$$

obtained quantum-mechanically by Gell-Mann.¹⁹ (This last expression holds only for small r_s , and has probably

¹⁹ M. Gell-Mann, Phys. Rev. **106**, 369 (1957).

been used to values of r_s larger than those for which it is valid.)

At $r_s = 4.3$, the equilibrium density for zero temperature, the specific heat is 0.80 of the Sommerfeld value for all temperatures from zero up to about $kT = \frac{1}{2}$ eV ($T \cong 6000^\circ\text{K}$). The DHTF theory thus predicts zero-temperature electronic energies in fairly good agreement with the quantum mechanical results (Fig. 3) without the unsatisfactory behavior of the low-temperature specific heat which is introduced by the exchange term in the Hartree-Fock approximation ($C_v \propto T/\ln T$).⁹

5. CONCLUSIONS

The DHTF theory described above appears to give quite reasonable values of the *total* energy, pressure, and specific heat of an electron gas at all densities. The reason why this can be true even though exchange effects (statistical correlations) are not included explicitly is that for $r_s < 1$, the Fermi energy is much more important than the energy due to correlation effects (either statistical or electrostatic), whereas for $r_s > 1$, electrostatic effects automatically introduce sufficient correlation that the Pauli principle is essentially satisfied.

It must be admitted that the theory as presented above can claim no more than the intuitive justification which underlies the ordinary Thomas-Fermi theory of the atom. However, the calculated electron-density function $n(r)$ necessarily tends to the correct values zero and n_0 as r tends to zero and infinity, respectively,²⁰ and also has the correct form in the limit r_s equals infinity. This, of course, does not imply that the detailed form of $n(r)$ must be right for finite r_s , but it is unlikely that it is too far off as long as r_s is greater than one or two.

6. ACKNOWLEDGMENT

The authors would like to express their appreciation to Professor K. A. Brueckner for several helpful discussions.

²⁰ This contrasts with the Thomas-Fermi theory of the atom, where the electron density has the wrong behavior in the limit of both small and large r .